Quantum Time Signals in Living Beings

Brad Eckert

Abstract—Consciousness can be considered a physical process occurring inside and outside of time simultaneously, per spiritual traditions and modern QM theory, using two-dimensional time. In this model, quantum time emerges from non-local consciousness as it interacts with both worlds. The relationship between the time dimensions provides a mechanism for apparent noise arising from both our biological signaling and connection to a timeless divinity. We present an algorithm for the demodulation of ubiquitous white and pink noise, which could have hidden information content that instruments the mind-body landscape and the interaction of eternal consciousness with the physical world.

Index Terms—Tao, noise, quantum time, relative time, consciousness, QTDSP.

1 Two-Dimensional Time

According to many spiritual traditions, including those that rely on direct observation through meditation, the consciousness of humans, animals, and all living things is a combination of the finite and the infinite, existing both inside and outside of time. Allowing more than one dimension of time may support this view of life beyond the supposed material world. The existence of non-local mind effects, since they hold up under serious investigation [1], provides an impetus for the investigation of multi-dimensional time as an aspect of consciousness.

The Wheeler-DeWitt equation [2] attempts to combine mathematically the ideas of quantum mechanics and general relativity. One of its implications is the "problem of time", which is a conceptual conflict between general relativity (GR) and quantum mechanics (QM). Quantum mechanics regards the flow of time as universal and absolute, whereas general relativity regards the flow of time as malleable and relative.

According to Wheeler-DeWitt, an observer outside of the universe doesn't experience time. Page and Wootters [3] addressed this paradox (time *seems* real enough) by treating time as an emergent phenomenon resulting from quantum entanglement. Experiments [4] on entangled particles have bolstered the theory.

There are other takes on timeless universe models. Aharonov's two-state formalism of quantum mechanics has also been used [5] to propose emergence of time from a timeless unus mundus quantum-like space. Jianfeng Li provides a good overview [6] of quantum mechanical timeless consciousness. Ralph Abraham and Sisir Roy [7] have proposed a mathematical model for the quantum vacuum as a model of consciousness. In it, spacetime emerges from the subtle $akasha$ existing outside of space and time.

There are two distinct types of time: emergent time, which emanates from the structure of space-time and its metrics, and a causal time, indicating the flow from the past to the future [8]. The time domains relate the two models of Physics: QM and GR. Note that since quantum mechanical effects can happen in either time direction, emergent time can just as well flow from the future to the past.

In the interest of having a nomenclature for this paper, one dimension of time is the "quantum time" domain and the other is the "relative time" domain. So, *quantum time* and *relative time*.

The word *quantum* is used in the Bohmian sense. The Bohmian interpretation of quantum mechanics is non-local. Experiments in non-locality [9] find that the mind extends beyond the skull.

To please the poets, let's put an Eastern spin on these well-established fields:

- GR = Yang: Time is space
- QM = Yin: Time is consciousness

1.1 Quantum Time and Consciousness

In the field of "quantum biology", there are many examples of biological systems exploiting quantum effects. One could suppose that nature would evolve to use quantum time.

The physical vacuum, a substrate for quantum interactions, is a natural mechanism for biological systems to have evolved to utilize. This pantheistic view allows for consciousness as the ground state of being. Consciousness is the interaction between the physical vacuum and biology which facilitates communication at any physical scale, from DNA to species.

This provides a possible signaling mechanism for consciousness in beings such as paramecia or slime molds, which exhibit conscious behavior but are too small for consciousness to arise from the network effects of neurons or ganglia.

One way to relate the two time dimensions is with a scale-invariant geometry that exploits self-similarity. For it to be scale-invariant, we use an exponential growth model for quantum time.

$$\tau \propto e^{\epsilon t} \tag{1}$$

This exponential relationship between τ and t is a key enabler of signal transformations.

The mechanics of signal generation can be considered in the context of quantum time. This arrangement lends itself to information flow, utilized by nature, between the time and timeless domains.

Resonance is treated as a physical phenomenon occurring in quantum time τ. A resonant frequency in τ is equivalent to a frequency chirp in t. This dynamic emergence of time should produce small but detectable artifacts. The stream of consciousness is treated as emerging from a probabilistic field rather than time abruptly appearing from nothing.

Biological systems evolve to minimize the expenditure of energy. Resonances (field analogs of electrical and mechanical ringing) require a small energy input to keep them going, assuming a reasonably high Q. It stands to reason that biological systems would use field resonances in the physical vacuum (the exact nature of the field doesn't need to be understood) to transmit consciousness information efficiently.

In other words, there is a basis for the notion that "It's all vibrations" if the vibrations occur in quantum time such that their signal artifacts produce what looks like a noise spectrum. This is almost certainly an overly simplified view, but perhaps sufficient to reach low-hanging fruit. There could be other time dimensions at play or even backward time effects providing the excitation for the resonance. Since we're only looking for artifacts, the details aren't as important as verifying the existence of the artifacts in the first place.

We live in a world of electronic noise, much of which is not fully understood. By digitizing and processing this noise in warped time domains, consciousness information could conceivably be extracted from the resulting signals using traditional detection technologies.

2 Exponential Flicker Noise

Flicker noise (or 1/f noise), has a power spectrum proportional to $1/f^{\alpha}$, where α is between 0.7 and 1.4. It's a type of noise prevalent in many natural systems. Flicker noise [10] is seen in music, seismic data, EEG and ECG data, and electronic devices. Some of the more popular explanations for the 1/f spectrum are:

- A superposition of relaxation processes.
- Carrier mobility fluctuations through Coulomb scattering.
- Self-organized criticality in systems with extended spatial degrees of freedom.

There are a good number of hypotheses for 1/f noise, to which we add one more:

- The superposition of exponential chirps.

An exponential swept-sine signal with constant amplitude has a power spectrum [11] that is constant-slope (on a log-log plot) at roughly -6dB per octave, similar to a flicker noise power spectrum. This is independent of "warp factor" ω.

$$Signal \propto sin(k \cdot e^{\omega t}) \tag{2}$$

2.1 Exponential White Noise

White noise has a flat power spectrum. In a white noise model of quantum time, chirps start at (or pass through) 0 and asymptotically approach a final frequency as quantum time merges into relative time.

$$\frac{1}{\tau} \propto (1 - e^{-\epsilon t}) \tag{3}$$

In other words, the consciousness signal emerges from a domain of infinite time. The power drops off at the same rate frequency increases, resulting in a flat spectrum from DC to f_0.

$$f = f_0 \cdot (1 - e^{-\epsilon t}) \tag{4}$$

$$p = p_0 \cdot e^{-\epsilon t} \tag{5}$$

Suppose there is a pilot frequency f_0. The chirp would mix with carrier f_0 to produce a downward chirp (assuming the signal is moving forward in time) with power dropping with frequency, which flattens out the spectrum so it's still white. The resulting chirp signal is more practical to detect due to the shortness of the time that the chirp itself spends in a bandwidth that lends itself to detection.

The amplitude droop may be compensated for in the input warping stage. White noise follows the same rules as pink noise except for some spectral bias.

2.2 Chaotic Noise

As noted in Robert May's widely cited paper [12], complex dynamics can arise from simple first-order difference equations. For example, Eq. 6 has chaotic behavior when a is between 3.57 and 4.00.

$$X_{n+1} = aX_n(1 - X_n) \tag{6}$$

The power spectrum of Eq. 6 is whitish when in chaos. Since computer-generated pseudorandom numbers use this principle, their spectra could have similar dynamics that come into play when generating signals to test demodulation algorithms.

There are many other chaos generators. The same chaotic attractors at work in the relative time domain could have analogs in the quantum time domain. Perhaps the chaos when transformed could offer identifiable patterns.

2.3 Information in the Noise

Since chirps are bounded in time, a single chirp has a finite existence within a practical bandwidth. It corresponds to a discrete impulse in the relative time domain, or one symbol of information. The idea of consciousness as time quanta may be useful here. The act of being is a stream of consciousness that could have corresponding streams of pulse-coded information, a kind of informational counterpart to DNA. The impulse stream would be decoded for its information content.

The existence of self-similar exponential chirp patterns could also have nothing to do with consciousness (as it's commonly understood) if emergent time is intrinsic to nature. Although there are empirical models and many studies surrounding noise sources, there is no general theory that explains the widespread occurrence of 1/f noise. Such a situation demands more experimental studies of noise, which 2D time modeling would provide. If there's something there, it will shed light on theories of noise.

Or, they could have everything to do with consciousness. The mantras of "Om" and "Ma" are reminiscent of frequency chirps, with mouth resonances modeling the tonality. These could be the sounds of cosmic existence.

To establish a notation and unit of measurement for quantum frequency, let the "warp factor" ω be in units of e, the mathematical constant derived by Leonhard Euler in the 1720s, per unit time. The pronunciation may be "e's per second" for e/s, for example.

Note that 1.0 e/s is very close to twice the Golden Ratio ($\Phi = 1.618 : 1$), so one should be careful when making assumptions about Golden Ratio relationships in nature.

2.4 A Spiral Conceptual Model

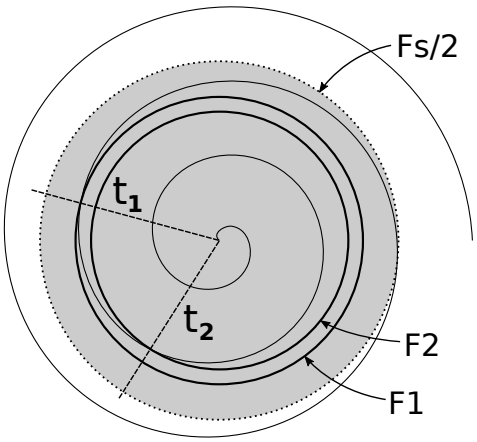

Fig. 1. Log polar plot of exponential chirp

Resonant signals in the quantum time domain could be re-mapped to relative time and demodulated by correlating a series of fast exponential chirp transforms. The spiral model needs ω to be real for Eq. 2 to be self-similar.

The correlation effect can be visualized as a spinning logarithmic spiral illuminated by a strobe light. When the strobe frequency matches the rate constant of the spiral(s), it appears to be standing still. Otherwise, it's a blur.

The relationship between quantum time and relative time can be thought of as a 2D plot in log-polar format. Log-polar format renders a logarithmic spiral as a linear (Archimedean) spiral. The spiral's radius is $\rho = k\theta$, where k is a rate constant. ρ can represent either time or frequency by flipping the sign of k. For purposes of signal processing, let ρ represent log frequency and θ relative time.

Log-polar mapping has proven useful in machine vision [13] because it approximates the primate visual map [14]. Humans are visual thinkers, so their waking consciousness should map onto the log-polar structure of quantum time signaling.

Fig. 1 plots an exponential chirp in log-polar format. A line can be drawn outward from the center of the spiral, crossing it at multiple points. The line rotates clockwise (in the case of downward chirp) at a step size (from t_1 to t_2) corresponding to the oversampling rate. For example, if the oversampling rate is 36 (each input value is used 36 times), the step size is $10°$. Each angular sweep of the unit circle (beginning and ending at line t_1 or t_2) represents the input

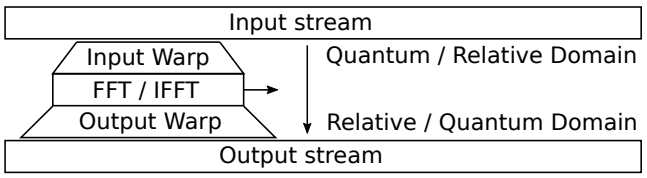

Fig. 2. Inter-domain data flow

to a version of the Mellin transform called the "Exponential Chirp Transform" (ECT) [13], which is basically a Fourier Transform with time-warped input.

The transform's frequency domain output is along line t_1 or t_2 from approximately ρ = 0 to Fs/2, where Fs/2 (the Nyquist frequency) is shown by the dashed circle. The radius of the circle represents the approximate bandwidth of the system. Not all of the circle is used: Anti-aliasing cuts off before Fs/2, while signal near the center is too spread out to be useful.

The ECT time-warps the chirp signal, which represents a single "quantum tone". In the $360°$ sweep at line t_1, the chirp is time-warped to a tone F1 in relative time. A time $t_2 - t_1$ later, at line t_2, it's time-warped to a tone of frequency F2. Time warping is exponential. Note that "exponential time warping" is different from "dynamic time warping", a popular means of pattern-matching mostly linear signals.

A convenient side effect of time warping is to transform interference (periodic signals) into wideband noise. The usual frequency peaks of EEG and HRV are thus reduced. Periodic signals could be notched out as needed by appropriate filters to further reduce their interfering effect.

Being logarithmic, quantum time has the property of frequency going as $-\tau$ rather than $1/t$. To change between time and frequency, just flip the sign of the exponent. Tones are mirror images of time. Signal processing is more convenient in terms of frequency, so that is the focus of this paper.

2.4.1 The Spiral Transform

The basic data flow of signal conversion from one time domain to another ($\tau \leftrightarrow t$) is shown in Fig. 2. The conversion algorithm slides along the input and output data streams, forward in time. Data is processed in overlapping chunks. In other words, after a block of processing, the sliding part of Fig. 2 shifts slightly to the right. In proportion to the amount of shift, new input stream is exposed and new output stream is sent out. The I/O streams are low-bandwidth compared to the compute-intensive processing block.

There are two use cases: demodulation and modulation. For demodulation ($\tau \rightarrow t$), the input stream is in the quantum time domain and the output stream is in the relative time domain. The input stream consists of real numbers. It gets exponentially time-warped to convert chirps to tones and fed through a FFT (Fast Fourier Transform). The FFT result is linearized with respect to the quantum domain by exponentially warping it and accumulating it in a correlator to include many instances of the same incoming chirp.

For modulation ($t \rightarrow \tau$), the input stream is in the relative time domain and the output stream is in the quantum time domain. It's the demodulation process in reverse. The usual use case is demodulation, so that will be the focus of the paper.

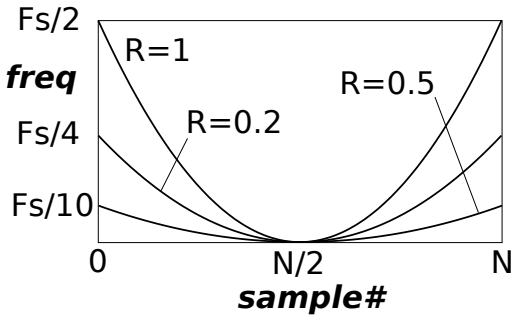

Fig. 3. Chirp Frequency in Parabolic Time

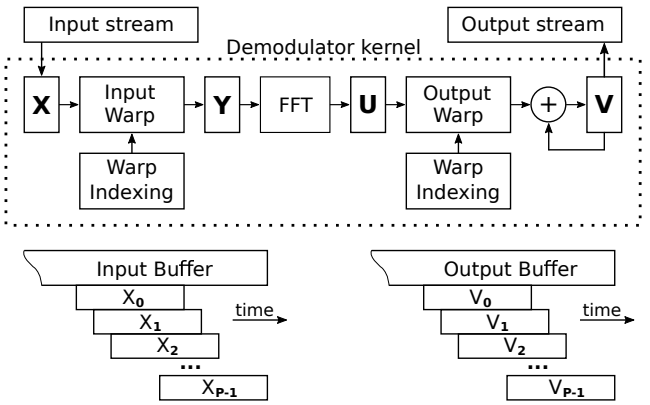

Fig. 4. Demodulation data flow

2.5 A Parabolic Conceptual Model

It's instructive to consider the case where ω is imaginary. The chirp frequency follows a cosine function (see Euler's Formula). Supposing the existence of a high frequency pilot tone $f_0 \gg F_S/2$ mixing with the chirp, the resulting frequency would follow a parabolic path down to 0 and back up again.

The parabolic model allows independence from the arrow of time since x^2 is symmetric in x. You would expect such independence in quantum time. A τ/t singularity occurs at "the now" in Eq. 7, which I call "the dharma point" because it merges with eternity. With an amplitude that goes as $\sqrt{|t - t_{now}|}$, the spectrum is white.

$$f(t, t_{now}) = k \cdot (t - t_{now})^2 \tag{7}$$

A problem with this model is that the cosine is periodic. If signals were present, one would expect periodic artifacts that would have been detected by now. Frequency analysis of noise from 10^{-6} Hz to over 1 THz can be found in the literature. However, it's only a problem if the chirp is repeating in the same timeline. The chirps could be on uncorrelated timelines. A chirp would only be detectable if its timeline enters the realm of phenomena that actually occur. Considering outcomes as arising from probablistic fields, the most likely probabilities should produce the strongest signals. Each chirp could be imagined as a conic section intersecting the light cones of a Minkowski Space Time diagram. Whether the conic section is parabolic, hyperbolic or elliptical, within the system passband (which is assumed to be very limited) it looks parabolic.

A spectrum analyzer for the parabolic model is simpler than one for the spiral model. The frequency chirps shown in Fig. 3 is time-warped by re-sampling so as to shift the frequencies up to their respective $F_S/2$, $F_S/4$, and $F_S/10$. This is fed through a Fourier Transform to produce a new column of pixels for each new slice of raw input data.

2.5.1 The Parabolic Transform

Since parabolic resampling shifts frequencies upward, a digital low pass filter must be applied to the data to avoid artifacts beyond $F_S/2$. Decimation factor m is 1 at the endpoints and 0 at the dharma point.

It's not feasible to resample the entire parabola. Resampling the parabola segment between $x = 0.5$ and $x = 1$ (or $x = -1$ and $x = -0.5$) allows $2N$ input samples to map to N time-warped samples. Decimation factor m ranges from 0.25 to 1 while the resample pitch ranges from 1 to 4.

The dharma point is N samples away from the resampled half-parabola. It's possible to run m all the way to 0, at the dharma point. The output of the digital filter is frozen in time at that point. Plotting the sequence of dharma points may be instructive.

A couple of stages of biquad low-pass filter serves to filter the input for up-sampling. Coefficients may be stored in a table of $4N$ sets of filter coefficients.

3 Spiral Model Demodulation

The mathematics of signal conversion, besides FFT, is mainly College Algebra. The algorithm can be coded by a typical programmer or engineer with the help from some math tricks and perhaps working around the bugs in my thinking.

3.1 Reference Chirp

The most important part of a software ecosystem is its test code. The test code for QTDSP generates a reference chirp. That chirp is the basis for the demodulation algorithm.

Let R be a scaled version of ω. Let N be the size of the Fourier Transform, which is an exact power of two. Typically, it's between 256 and 16384. Stepping n from 0 to N-1,

$$f(n) = f_0 \cdot exp\left(\frac{nR}{N}\right) \tag{8}$$

Computing many sequential points of transcendental functions tends to be slow. It's better to come with a fast algorithm. With some luck, it will also illuminate the problem of fast signal demodulation.

Stepwise exponential growth or decay can be handled by a multiply operation. Let b be the step size for the multiplier. Setting $e^R = (1 + b)^N$,

$$b = e^{R/N} - 1 \tag{9}$$

For each iteration:

$$f_{n+1} = f_n \cdot (1 + b) \tag{10}$$

Since $R/N \ll 1$, the first term or two of the Maclaurin series expansion of the exponent function is enough for a good approximation. So, b is very close to R/N.

3.2 Input Warping

The downsampling process of Fig. 4 translates the sample pitch of $\boldsymbol{X}$ to the sample pitch of $\boldsymbol{Y}$ using an exponential sweep. In the industry, this is known as exponential time-warping. The input time warp re-samples input data such that a reference chirp would get translated to a constant-period sinusoid.

An exponential chirp sweeps from f_0 to f_1 in a time t. M points of $\boldsymbol{X}$ get mapped onto N points of $\boldsymbol{Y}$, where $M < N$. Re-sampling is done on N points (of $\boldsymbol{Y}$) at a time where the respective indices of $\boldsymbol{X}$ and $\boldsymbol{Y}$ are δ and i. $\boldsymbol{X}$ is swept from $\mathbf{X}_0$ to $\mathbf{X}_M$ or $\mathbf{X}_M$ to $\mathbf{X}_0$.

Let λ be the sample pitch of $\boldsymbol{X}$. It will increase or decrease exponentially and should have a maximum value of 1.

This causes a chirp of matching R to be re-sampled to the upper frequency (either f_0 or f_1 depending on the sign of R). Given output index i, input sample index $\delta(i)$ is the accumulated sum of $pitch(i)$ where $pitch$ decreases exponentially from 1.0 or increases exponentially toward 1.0. In the latter case, the initial $pitch$ can either be determined from a dummy run of the resampling algorithm or analytically. It's $e^{M \cdot R/N}$. M is derived from a geometric progression in Eq. 11.

$$N = \sum_{k=1}^{M} e^{|R| \cdot (k-1)/N} = \frac{1 - e^{|R| \cdot M/N}}{1 - e^{|R|/N}} \tag{11}$$

$$M = \frac{N}{|R|} \cdot \ ln\left(1 - N(1 - e^{|R|/N})\right) \tag{12}$$

An analytical expression of the re-sampling function (i to δ) was over my head, but it's easily expressed as an algorithm. Interpolating from a fractional $\boldsymbol{X}$ index in this example (WarpIn listing) is done by cubic interpolation using a Catmull-Rom spline. Given four points y_0, y_1, y_2, y_3, a cubic polynomial describes the curve passing through all four points whose slope matches up between adjacent segments. With x ranging from 0 to 1 indexing the point on $[y_1, y_2]$.

$$f = a_0 \cdot x^3 + a_1 \cdot x^2 + a_2 \cdot x + a_3 \tag{13}$$

Regardless of the sign of R, the input warp shifts the corresponding chirp to the lesser of f_0 and f_1. Let γ be the highest frequency component in the time-warped input:

$$\gamma = \frac{N}{2} \cdot \frac{1}{1 + |R|} \tag{14}$$

Note: The effect of S on γ hasn't been tested yet.

Input interpolation produces noise artifacts, as you would expect. They get spread broadly across the spectrum above the region of interest. Figure 5 shows the output power spectrum (10 dB/div) of the warp function. The test chirp decays in frequency exponentially from $0.45F_S$ with $R = -2$. A 4096-point Fast Fourier Transform omits the window function so you can see the distribution of noise artifacts to the right of the peak.

That's a great relief because it removes any need for much more compute-intensive resampling algorithms. Warping may be kept simple and fast.

```
float WarpIn(
  float* out,    // output stream
  float* in,     // input stream
  int length,    // points in output stream
  double delta,  // starting input index, 0 to 1
  double pitch,  // exponential input sample pitch
  double b,      // exp rate of change of pitch
  double amplitude, // starting amplitude
  double fcomp)  // decay rate of amplitude
{
  float y0 = *in++;
  float y1 = *in++;
  float y2 = *in++;
  float y3 = *in++;
  // coefficients for first y1-y2 segment of the curve
  float a0 = -0.5 * y0 + 1.5 * y1 - 1.5 * y2 + 0.5 * y3;
  float a1 = y0 - 2.5 * y1 + 2.0 * y2 - 0.5 * y3;
  float a2 = -0.5 * y0 + 0.5 * y2;
  float a3 = y1;
  for (int i = 0; i < length; i++) {
    float x = delta; // between 0 and 1 on y1-y2 path
    float sum = x * (x * (x * a0 + a1) + a2) + a3;
    *out++ = sum * amplitude; // deemphasize low end
    delta += pitch;
    if (delta >= 1.0) {
      delta -= 1.0;
      pitch += pitch * b;
      amplitude += amplitude * fcomp;
      y0 = y1;    // stepped into the next segment
      y1 = y2;
      y2 = y3;
      y3 = *in++;
      a0 = -0.5 * y0 + 1.5 * y1 - 1.5 * y2 + 0.5 * y3;
      a1 = y0 - 2.5 * y1 + 2.0 * y2 - 0.5 * y3;
      a2 = -0.5 * y0 + 0.5 * y2;
      a3 = y1;
    }
  }
  return pitch;
}
```

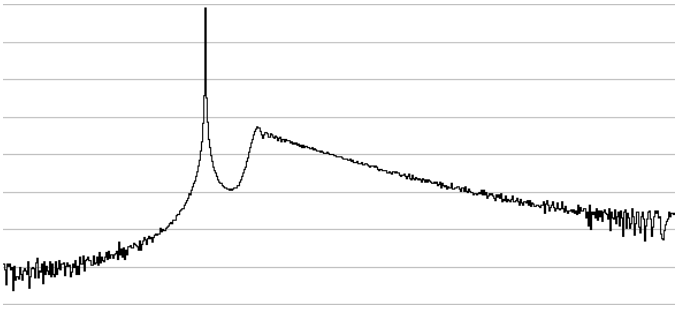

Fig. 5. f_1 peak of warped exponential chirp, with artifacts.

3.3 FFT

After $\boldsymbol{X}$ is time-warped into $\boldsymbol{Y}$, $\boldsymbol{Y}$ is processed by a Fast Fourier Transform and converted to data set $\boldsymbol{U}$ containing N/2 frequency bins. Not all of them are used. Outputs above γ (Eq. 14) are ignored.

$\boldsymbol{Y}$ and $\boldsymbol{U}$ may share the same physical memory if the FFT is performed in place. The output of the FFT is converted to the square of the magnitude for use in RMS averaging, so square root is not needed.

A window function $w(n)$ is applied to Y before performing the FFT. Hann and Nuttall windows are both good functions, with a tradeoff between peak spreading and dynamic range. Eq. 15 is the Hann window function.

$$w(n) = \frac{1}{2}\left(1 - cos\left(\frac{2\pi n}{N-1}\right)\right) \tag{15}$$

```
static void WarpOut(
  float* out,         // output stream (V)
  float* in,          // input stream (mag^2)
  int length,
  double gamma,       // max epsilon index
  double zeta,        // rate of change of gamma
  float fcomp)        // decay rate of amplitude
{
  int idx0 = (int)gamma;
  in = &in[idx0 + 1]; // -> first point
  double epsilon = gamma;
  float amplitude = 1.0f;
  float y1 = *in--;
  float y0 = *in--;
  float a0 = y1 - y0;
  float a1 = y0;
  for (int i = 0; i < length; i++) {
    float idx1 = idx0;
    float x = gamma - idx0; // between 0 and 1 on y0-y1
    float sum = x * a0 + a1;
    *out++ = sum * amplitude; // deemphasize low end
    amplitude += amplitude * fcomp;
    gamma += gamma * zeta; // epsilon exponentially decays
    idx0 = (int)gamma;
    if (idx0 != idx1) {
      y1 = y0;          // stepped into the next segment
      y0 = *in--;
      a0 = y1 - y0;
      a1 = y0;
    }
  }
}
```

Given N input points, output indices up to $\frac{0.5 \cdot N}{1+|R|}$ are used for further processing.

3.4 Output Warping

$\boldsymbol{U}$ is upsampled to form time-domain signal $\boldsymbol{V}$. Let ϵ and j be the respective indices of $\boldsymbol{U}$ and $\boldsymbol{V}$. The maximum usable value of ϵ is γ (Eq. 14). Integer index j steps one at a time while ϵ decays exponentially.

Warp indexing uses the relation:

$$\epsilon = \gamma e^{\omega(t-\tau)} \tag{16}$$

Time t (scaled to match the output stream's sample rate) sweeps from τ in the opposite direction of R's sign, causing the exponent to start at 1 and decay downward.

j sweeps downward from $\gamma(N/2-1)$. Index $\epsilon(j)$ is independent of R.

$$\epsilon(j) = \gamma e^{-kj/N} \tag{17}$$

The desired difference between $\epsilon(0)$ and $\epsilon(1)$ in Eq. 17 is 1. $\epsilon(0) = \gamma$ and $\epsilon(1) = \gamma e^{-k/N}$, which gives a k of about $-2|R|$:

$$k = N \cdot ln\left(1 - 2 \cdot \frac{|R|+1}{N}\right) \tag{18}$$

The exponential decay of ϵ can be handled by repeated multiplication, one per $\boldsymbol{U}_\epsilon$ fetch. The exponential sweep needs a small correction factor to have a base of exactly e. Setting $e^k = (1+\zeta)^N$,

$$\zeta = e^{k/N} - 1 \tag{19}$$

Sample C code for the output warp:

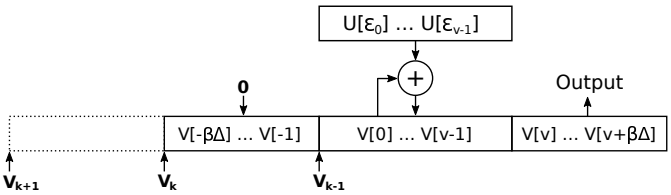

Fig. 6. Correlation of $\boldsymbol{V}$

3.5 Correlation

Let H_X be the integer number of new X samples per conversion.

Let H_V be the real number of output samples per conversion. Combining Eq. 14 and Eq. 18 gives:

$$H_V = H_X \cdot \frac{R}{N} \cdot \frac{R}{|R|+1} \cdot \frac{-1}{ln(1-\frac{2|R|}{N})} \tag{20}$$

Since ϵ is always positive, the upchirp case of $R > 0$ needs to have its j index mirrored by using $\boldsymbol{U}_{v-j}$, where v is the maximum j such as (15/32)N. The warp output is added to $\boldsymbol{V}$ memory as described below, indexed from the top or bottom of the active region of V.

Warped $\boldsymbol{U}$ is added to output buffer $\boldsymbol{V}$ by summation, staggered in time (by H_V samples) for each processing block. When the downsampler's R value matches the chirp rate of an incoming chirp, multiple peaks in the warped FFT output correlate in the output stream to produce a corresponding output pulse in the $\boldsymbol{V}$ stream. A more complex signal such as overlapping and/or modulated chirps will produce pulse trains and/or modulation envelopes in the $\boldsymbol{V}$ stream.

$\boldsymbol{U}$ is in logarithmic format so that summing a bunch of them is basically repeated multiplication. It's cheaper than actual multiplication and less subject to overflow. Multiplying (or summing logs) of linearized spectra is a form of cross-correlation. The sum can be normalized with a scale that's the inverse of the V oversampling:

$$scale = -H_X \cdot \frac{R^2}{ln(1-\frac{2|R|}{N})} \tag{21}$$

Fig. 6 shows the output correlator, another view of buffer $\boldsymbol{V}$. The output stream flows from left to right, being initialized to 0 outside the accumulation region. After U_ϵ is added to $\boldsymbol{V}$, the V_0 index moves H_V points to the left, leaving H_V newly minted output points.

Elements of $\boldsymbol{V}$ are accumulated squares of magnitudes. An attempt was made to accumulate vectors, with the idea that the phase rotations might sync up, but it didn't work in simulation. So, angle data from the FFT is discarded.

4 Parabolic Model Demodulation

The parabolic time model is simpler than the spiral model. There's no correlator. A spectrum analyzer is also easier to build.

4.1 Reference Chirp

The parabolic chirp has a frequency that starts at F_0 and ends at 0. Its frequency forms half of a parabola when N points are plotted.

```
void ParabolicWarp(
  float* out,   // output stream
  float* in,    // input stream
  int n,        // points in output stream
  float pitch)  // exponential input sample pitch
{
  float y0, a0, a1, a2, a3;
  float y1 = *in++;
  float y2 = *in++;
  float y3 = *in++;
  float x = 0;  // between 0 and 1 on y1-y2 path
  float dp = n; // dharma point is at right edge
  float dp0 = sqrtf(pitch) * dp;
  pitch = 1.0;
  for (int i = 0; i < n; i++) {
    x += pitch;
    if (x >= 1.0) { // stepped into the next segment
      x -= 1.0;
      float s = dp0 / dp;
      pitch = s * s;
      dp--;
      y0 = y1;
      y1 = y2;
      y2 = y3;
      y3 = *in++;
      // coefficients for y1-y2 segment of the cubic curve
      a0 = -0.5f * y0 + 1.5f * y1 - 1.5f * y2 + 0.5f * y3;
      a1 = y0 - 2.5f * y1 + 2.0f * y2 - 0.5f * y3;
      a2 = -0.5f * y0 + 0.5f * y2;
      a3 = y1;
    }
    *out++ = x * (x * (x * a0 + a1) + a2) + a3;
  }
}
```

4.2 Input Warping

The downsampling process of Fig. 4 translates the sample pitch of $\boldsymbol{X}$ to the sample pitch of $\boldsymbol{Y}$ using a parabolic sweep. The input time warp re-samples input data such that a reference chirp would get translated to a constant-period sinusoid.

M points of $\boldsymbol{X}$ get mapped onto N points of $\boldsymbol{Y}$, where $M = 0.468N$. The chirp's F_0 gets down-sampled by a factor of 3.53 to match F_1, the frequency at $X[M]$. As with the spiral model, such down-sampling is well-behaved. Upsampling F_1 to F_0 would be more difficult and need anti-aliasing filtering.

Rather than showing a mathematical derivation, a code listing of the time warping tells all. Cubic interpolation via Catmull-Rom spline is again used.

After $\boldsymbol{X}$ is time-warped into $\boldsymbol{Y}$, $\boldsymbol{Y}$ is processed by a Fast Fourier Transform and converted to magnitude data $\boldsymbol{U}$ containing N/2 frequency bins. Not all of them are used. Outputs above $F_S/7$ are ignored.

Given N input points, output indices up to $F_S/7$ are used for further processing.

4.3 Spectral Display for Parabolic Time

The FFT output can be used to form a column of heat-mapped pixels on a display. Each subsequent conversion forms another column. H_X samples are appended to $\boldsymbol{X}$ for each new conversion. A GPU would typically run hundreds of warps and FFTs in parallel to produce a 2D image as a single processing block.

Since there is no correlation step, the parabolic chirp is smeared across the output image. Figure 7 illustrates the image produced by a test waveform. F_0 is $F_S/2$. At F_0, the smear is thinnest. The high frequency components of the smear are the most pronounced at F_0. A 2D FFT can be used to help pick out the location of the chirp.

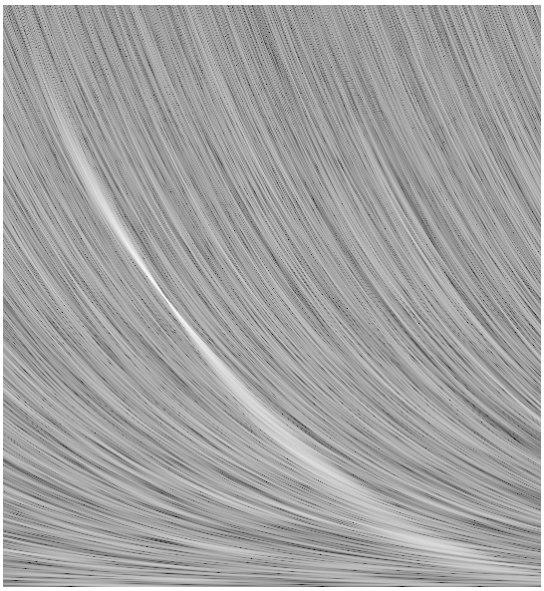

Fig. 7. Parabolic chirp 3dB below noise.

5 Testing the Demodulator

The demodulation algorithm was tested by coding the algorithm in C. The test app uses OpenGL and GLFW3 to provide a user interface and NVIDIA's CUDA SDK to provide DSP power for the transform.

The software has a dependency on NVIDIA GPU cards. The magic of GPUs lies in an architecture that efficently streams DRAM bursts into and out of many CPU cores that operate in parallel. The application operates on many values of R concurrently. The development PC had a GTX 1080 graphics card. Newer graphics cards such as the GTX 1660 ti offer nearly the same performance at much lower cost: The DRAM bus isn't as wide but it uses a faster clock. Look for a wide (such as 192-bit) memory bus and GDDR6.

With the GTX 1080, the CUDA-based algorithm was about 15 times as fast as an FFTW-based version running on a single thread of a 3 GHz CPU core. Running the algorithm in many threads on an expensive CPU could bring the performance more in line with GPU performance, but more likely is that memory bandwidth limitations will keep a CPU-based solution slower than the GPU-based version. Some of the higher end GPUs use stacked-die memory to provide much higher bandwidth, so GPUs provide a real performance upgrade path.

The spectrogram consists of a range of R values spread vertically with time on the horizontal axis. Since the number of output points vary with R, time is normalized to the left edge of the image. At the left edge, the same amount of total time has elapsed for each row of pixels.

5.1 Spectrogram of a test chirp

Figure 8 shows a spectrogram image of a noisy negative-chirp (R = -0.5) test signal with R on the vertical axis. $R = -0.4$ is at the top and $R = -0.6$ is at the bottom. A test

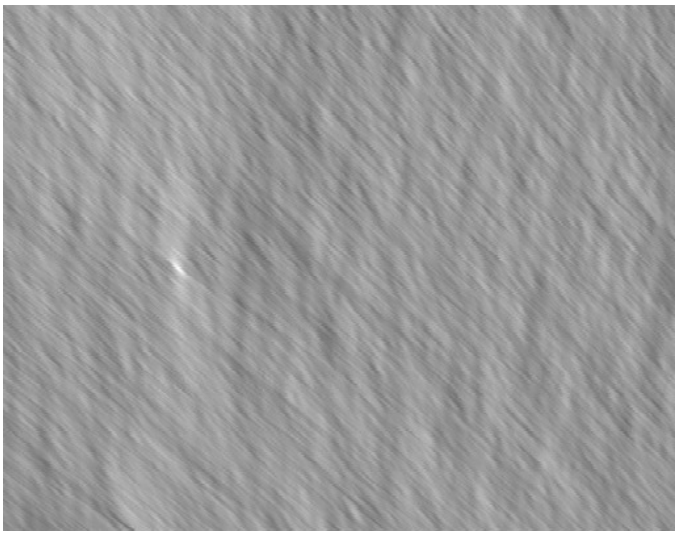

Fig. 8. Chirp power $(R < 0)$ 20dB below noise.

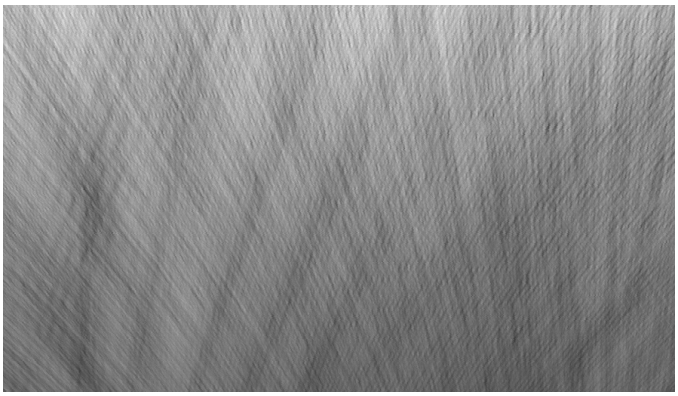

Fig. 9. Bach's Toccata and Fugue in D minor.

signal was used to demonstrate detection of a chirp at $R = -0.5$ and $N = 4096$. The chirp amplitude is $1/10$ of the noise amplitude.

The noise produces a kind of slate or sandstone texture. The white spot is the test chirp. An oversample factor of 64 seems to be optimal. Oversampling is the number of times an X input point is used in overlapping operations. For example, 64 new input points for N = 4096. Lower oversample factors leave more visible (patterned) artifacts. Higher ones produce about the same smoothness with more computation load. They don't really increase sensitivity. Higher N mostly increases resolution and to some extent sensitivity.

White, pink, and brown noise (without the test chirp) has about the same appearance noted above.

5.2 Spectrogram of music

The first 2.5 minutes of Bach's Toccata and Fugue in D minor seemed like a good test of tone-rich music. Organ notes are rich in harmonics. The other test was the Surfaris "Wipe Out", another instrumental piece with rich harmonics. Both were resampled to 22050 SPS.

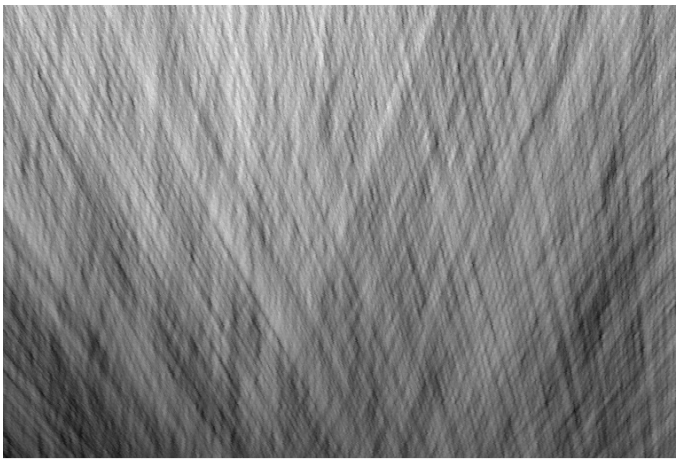

Fig. 10. The Surfaris Wipe Out.

Fig. 11. EEG of a test subject in stage 2 sleep.

Figure 10 illustrates the texture of a periodic waveform. Tones appear as wideband noise in the FFT output. They can produce wide but faint lines in the output.

5.3 Spectrogram of an EEG signal

EEG data was downloaded from the Sleep Spindles Database, excerpt 2. Its web link is broken, but the data is in the wild. Figure 11 shows the spectrogram during stage 2 sleep.

The spectrogram looks different from synthetic noise. It has the slate-like texture of synthetic noise but with "scratches" and "hair" that give a different appearance.

Although visual interpretation at this point is like reading tea leaves, a trend that seems to be at play is that the warp factor, ω, is not constant. It changes exponentially, forming sloped (but mostly straight) lines in the output. These lines overlap in time and have different slopes. Sometimes the slope shifts from positive to negative, through vertical. Sometimes it seems a line with a slope will have a line near it with the sign of its slope flipped.

The exponential emergent time model is much more complex than initially thought. You would think we were dealing with nature. The signals we're looking at aren't self-similar fractals. The most computationally feasible means of decoding is probably to stick with the exponential chirp transform model and post-process the 2D spectral image.

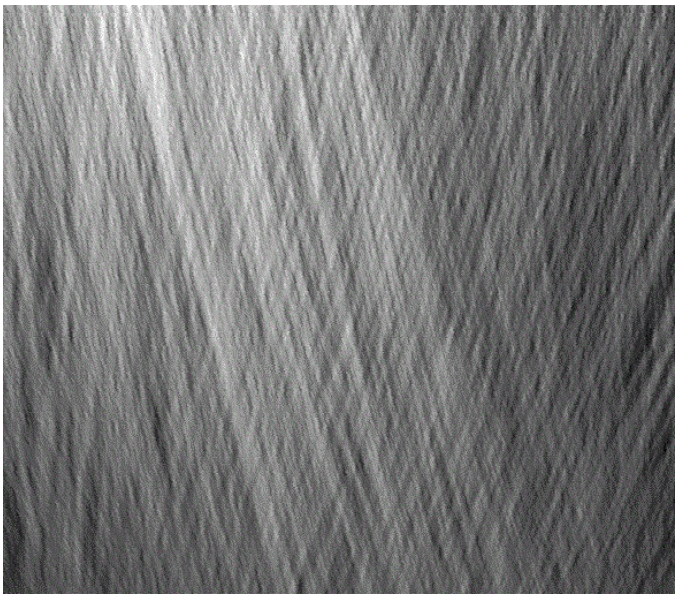

Fig. 12. EEG of a test subject waking up from sleep for about 30 seconds.

The transform depends on self-similarity in the time warping, which seems to limit it to a power function.

Rather than "fix" the transform, it should be easier to look for lines in the spectrogram. It may be useful to keep in mind that an FM-modulated signal will produce multiple parallel lines. The intensity of the lines would be reminiscent of the frequency spectrum of a typical FM signal.

6 Summary

Signals that appear to be pure noise may contain hidden signals regarding non-local consciousness. These signals could be analyzed to "instrument the soul". Follow-up work to be done includes:

- Add features to the QTSA app to facilitate signal identification.
- Analyze existing experimental data to search for new signals.
- Develop new sensor technologies using quantum and spin effects.

The social impetus for such work is to repair the dysfunction introduced by new technologies such as social media and pseudo-anonymous communications. Instrumenting the soul would provide a new way of interacting that is completely open and honest. Solving the trust problem would be a boon to economies across the globe.

References

[1] E. F. Kelly, *Irreducible Mind: Toward a Psychology for the 21st Century*. Rowman and Littlefield, 2009.

[2] B. S. Dewitt, "Quantum theory of gravity. i. the canonical theory," *Physical Review*, vol. 160, pp. 1113–1148, 1967, doi:10.1103/PhysRev.160.1113.

[3] D. N. Page and W. K. Wootters, "Evolution without evolution: Dynamics described by stationary observables," *Physical Review D*, vol. 27, no. 12, pp. 2885–2892, 1983.

[4] E. M. et al., "Time from quantum entanglement: an experimental illustration," *Physical Review A*, vol. 89, 2014, 052122.

[5] A. C. Lobo, "Time and consciousness in a quantum world," 2017.

[6] J. Li, "A timeless and spaceless quantum theory of consciousness," *NeuroQuantology*, vol. 11, pp. 431–442, 2013.

[7] S. Roy and R. Abraham, *DEMYSTIFYING THE AKASHA Consciousness and the Quantum Vacuum*, 01 2011.

[8] O. Brunet, "Geometric time and causal time in relativistic lagrangian mechanics," 2016.

[9] e. a. Jeanne Achterberg, "Evidence for correlations between distant intentionality and brain function in recipients: A functional magnetic resonance imaging analysis," *Journal of Complementary and Alternative Medicine*, vol. 11, no. 6, pp. 965–971, 2005.

[10] E. Milotti, "1/f noise: a pedagogical review," 2002.

[11] A. N. et al, "Nonlinear system identification using exponential swept-sine signal," *IEEE Transactions on Instrumentation and Measurement*, vol. 59, no. 8, pp. 2220–2229, 2010, doi:10.1109/tim.2009.2031836.

[12] R. M. May, "Simple mathematical models with very complicated dynamics," *Nature*, vol. 261, pp. 459–467, 1976, doi:DOI: 10.1038/261459a0.

[13] G. Bonmassar and E. L. Schwartz, "Space-variant fourier analysis: the exponential chirp transform," *IEEE Transactions on Pattern Analysis and Machine Intelligence*, vol. 19, pp. 1080–1089, 1997, DOI:10.1109/34.625108.

[14] E. L. Schwartz, "Cortical anatomy, size invariance, and spatial frequency analysis," *Perception*, vol. 10, pp. 455–469, 1981.